the plant journal

SEB SOCIETY FOR EXPERIMENTAL BIOLOGY

The Plant Journal (2010) **62**, 713–725 doi: 10.1111/j.1365-313X.2010.04183.x

ZEBRA-NECROSIS, a thylakoid-bound protein, is critical for the photoprotection of developing chloroplasts during early leaf development

Jinjie Li[1,2,†], Devendra Pandeya[1,†], Krishna Nath[3,†], Ismayil S. Zulfugarov[3,4], Soo-Cheul Yoo[1], Haitao Zhang[1], Jeong-Hoon Yoo[1], Sung-Hwan Cho[1], Hee-Jong Koh[1], Do-Soon Kim[1], Hak Soo Seo[1], Byoung-Cheorl Kang[1], Choon-Hwan Lee[3,*] and Nam-Chon Paek[1,*]

[1]*Department of Plant Science, Plant Genomics and Breeding Institute, and Research Institute for Agriculture and Life Sciences, Seoul National University, Seoul 151-921, Korea,*

[2]*Key Laboratory of Crop Genomics and Genetic Improvement of Ministry of Agriculture and Beijing Key Lab of Crop Genetic Improvement, China Agriculture University, Beijing 100094, China,*

[3]*Department of Molecular Biology, Pusan National University, Busan 609-735, Korea, and*

[4]*Institute of Botany, Azerbaijan National Academy of Sciences, Baku AZ 1073, Azerbaijan*

Received 10 January 2010; revised 6 February 2010; accepted 12 February 2010; published online 25 March 2010.
*For correspondence (fax +82 2 873 2056; e-mail chlee@pusan.ac.kr, ncpaek@snu.ac.kr).
†These authors contributed equally to this work.

SUMMARY

The *zebra-necrosis* (*zn*) mutant of rice (*Oryza sativa*) produces transversely green/yellow-striped leaves. The mutant phenotype is formed by unequal impairment of chloroplast biogenesis before emergence from the leaf sheath under alternate light/dark or high/low temperatures (restrictive), but not under constant light and temperature (permissive) conditions. Map-based cloning revealed that *ZN* encodes a thylakoid-bound protein of unknown function. Virus-induced gene silencing of a *ZN* homolog in *Nicotiana benthamiana* causes leaf variegation with sporadic green/yellow sectors, indicating that ZN is essential for chloroplast biogenesis during early leaf development. Necrotic lesions often occur in the yellow sectors as a result of an excessive accumulation of reactive oxygen species (ROS). The phenotypic severity (leaf variegation and necrosis) and ROS levels are positively correlated with an increase in light intensity under restrictive conditions. In the mutant leaves, chlorophyll (Chl) metabolism, ROS scavenging activities, maximum quantum yield of photosystem II (PSII), and structures and functions of the photosynthetic complexes are normal in the Chl-containing cells, suggesting that ROS are mainly generated from the defective plastids of the Chl-free cells. The PSII activity of normal chloroplasts is hypersensitive to photoinhibition because the recovery rates of PSII are much slower. In the PSII repair, the degradation of damaged D1 is not impaired, suggesting a reduced activity of new D1 synthesis, possibly because of higher levels of ROS generated from the Chl-free cells by excess light. Together, we propose that ZN is required for protecting developing chloroplasts, especially during the assembly of thylakoid protein complexes, from incidental light after darkness.

Keywords: Zebra-Necrosis, leaf variegation, chloroplast biogenesis, ROS, photoinhibition.

INTRODUCTION

During photomorphogenesis of the shoot organs of higher plants, plastid differentiation from nonfunctional proplastids to photosynthetically active chloroplasts is accomplished by the formation of thylakoid membranes, and the assembly of thylakoid-bound protein complexes, including photosynthetic apparatus (Surpin *et al.*, 2002; Zhang *et al.*, 2006).

Light is the sole energy source for photosynthesis, but ironically also causes constant damage to the photosynthetic complexes of chloroplasts. When the equilibrium of damage and repair in this machinery is disturbed by excess light, photoinhibition (or photoinactivation) of photosystem II (PSII) occurs. Photoinhibition is a complex process that includes photodamage to D1, new D1 synthesis for PSII repair, and reactivation of PSII function in the thylakoid membranes. In PSII repair, damaged D1 should be rapidly degraded by chloroplast proteases, and new D1 should be

reincorporated into the PSII complex (Aro *et al.*, 1993). Prolonged photoinhibition leads eventually to bleaching or necrotic lesions in the plant tissues as a result of an excessive accumulation of reactive oxygen species (ROS), reminiscent of a hypersensitive response (HR) reaction to pathogen infection (Overmyer *et al.*, 2003). In addition to D1 damage from photoinhibition, the PSII repair cycle is also negatively affected by external stress (Murata *et al.*, 2007; Takahashi and Murata, 2008).

In plants, ROS such as singlet oxygen, superoxide anion radicals and hydrogen peroxide (H_2O_2) are constantly produced in the chloroplasts, mitochondria and peroxisomes as by-products of aerobic reactions in several metabolic processes. When ROS production exceeds the scavenging capacity for these radicals under unfavorable biotic and abiotic stress, ROS act as cytotoxins to induce necrotic lesions, and also to alter the expression of certain genes in many signaling pathways, eventually leading to accelerated cell death (Ahmad *et al.*, 2008; Apel and Hirt, 2004). To prevent photooxidative damage, phototrophic organisms have evolved to possess several antioxidant enzymes, as well as repair machineries in the chloroplasts and cytoplasm. However, the developmental and genetic regulatory mechanisms for acquisition of a photoprotective capacity in the chloroplasts, particularly during chloroplast biogenesis, are largely unknown.

Leaf variegation has been identified in many species of higher plants, and this abnormal phenotype arises from the mutations of nuclear or plastid genes that impair chloroplast biogenesis (Aluru *et al.*, 2006). Variegated plants are easily distinguished by the green/white (or yellow) sectors of developing leaves. In most cases, the green sectors have almost the same levels of photosynthetic pigments in the chloroplasts of normal function, and the white (or yellow) sectors contain no chlorophyll (Chl) or carotenoids in either arrested or defective plastids (Kusumi *et al.*, 2000; Yu *et al.*, 2007; Yoo *et al.*, 2009). In contrast with albino mutants, variegated plants are maintained as homozygous because the green sectors provide sufficient levels of photosynthesis for their growth and reproduction (Sakamoto, 2003). The Arabidopsis *immutans* (*im*) mutant exhibits light-dependent leaf variegation resulting from an excessive accumulation of an intermediate precursor of carotenoids, phytoene (Aluru *et al.*, 2001, 2009), indicating that carotenoids are essential for chloroplast biogenesis by preventing photoinhibition during photosynthesis (Carol *et al.*, 1999; Wu *et al.*, 1999; Carol and Kuntz, 2001). The *fluorescent* (*flu*) mutant of Arabidopsis and the *tigrina* mutant of barley (*Hordeum vulgare*) have a defect in the Chl synthetic pathway, and, as a result, their leaves accumulate a phototoxic Chl precursor in darkness, protochlorophyllide (Pchlide), that leads to leaf bleaching under alternate light/dark cycles (Hansson *et al.*, 1997; Meskauskiene *et al.*, 2001). In contrast, lesion mimic mutants characterized by the spontaneous death of localized cells in their leaf tissues are thought to have defects in the regulation of programmed cell death processes, and often display a broad spectrum of resistance to fungal and bacterial diseases (Yamanouchi *et al.*, 2002; Kojo *et al.*, 2006). Moreover, both maize *lethal leaf spot 1* (*lls1*) and Arabidopsis *accelerated cell death 1* (*acd1*) mutants accumulate a phototoxic Chl intermediate: pheophorbide *a*. They display a spread of necrotic spots in mature leaves as a result of a loss of pheophorbide *a* oxygenase activity, which is responsible for Chl turnover (Pružinská *et al.*, 2003; Yang *et al.*, 2004). A mutation in *ACD2* encoding red chlorophyll catabolite reductase causes leaf bleaching as this enzyme can reduce a phototoxic Chl catabolism intermediate, and its loss results in an excess accumulation of ROS in the leaf tissues under exposure to light after a period of darkness (Yao and Greenberg, 2006; Pružinská *et al.*, 2007). A recent report has also shown that the imbalance between synthesis and degradation of proteins during photoinhibition leads to a permanent arrest of chloroplast biogenesis during early leaf development (Miura *et al.*, 2007).

Here, we show the phenotypic characteristics of a variegation/lesion mimic *zn* mutant of rice under field and growth chamber conditions, and the positional cloning of *ZN* that encodes a thylakoid-bound protein, the sequence and function of which are highly conserved in plants. Transverse green/yellow stripes on the mutant leaves are produced as a result of the random disability of chloroplast development before emergence from the leaf sheath under diurnal fluctuations of light/dark or high/low temperatures. Necrotic lesions often occur in the yellow sectors because of an excessive accumulation of ROS. The phenotypic severity and ROS accumulation are positively correlated with an increase in light intensity, and the PSII activity of the Chl-containing cells is hypersensitive to photoinhibition because of its slow recovery rate of PSII. This inefficient PSII repair appears to result from a retardation of the de novo synthesis of D1, possibly because of elevated levels of singlet oxygen that have been generated from the trace levels of free Chls in the yellow cells, by excess light. Taken together, we report that ZN is an essential thylakoid component of higher plants for protecting developing chloroplasts, possibly during the assembly of thylakoid protein complexes, under natural growth conditions.

RESULTS

Phenotypic characterization of the *zebra-necrosis* (*zn*) mutant of rice

Under field conditions, the *zn* mutant plants produce transverse striped leaves with the green (*zn*-G) and yellow (*zn*-Y) sectors, and necrotic lesions often occur in the *zn*-Y sectors during leaf elongation. This unusual phenotype is maintained in the leaf organs throughout development (Figure 1a). The yellow cross-bands (referred to as zebra stripes)

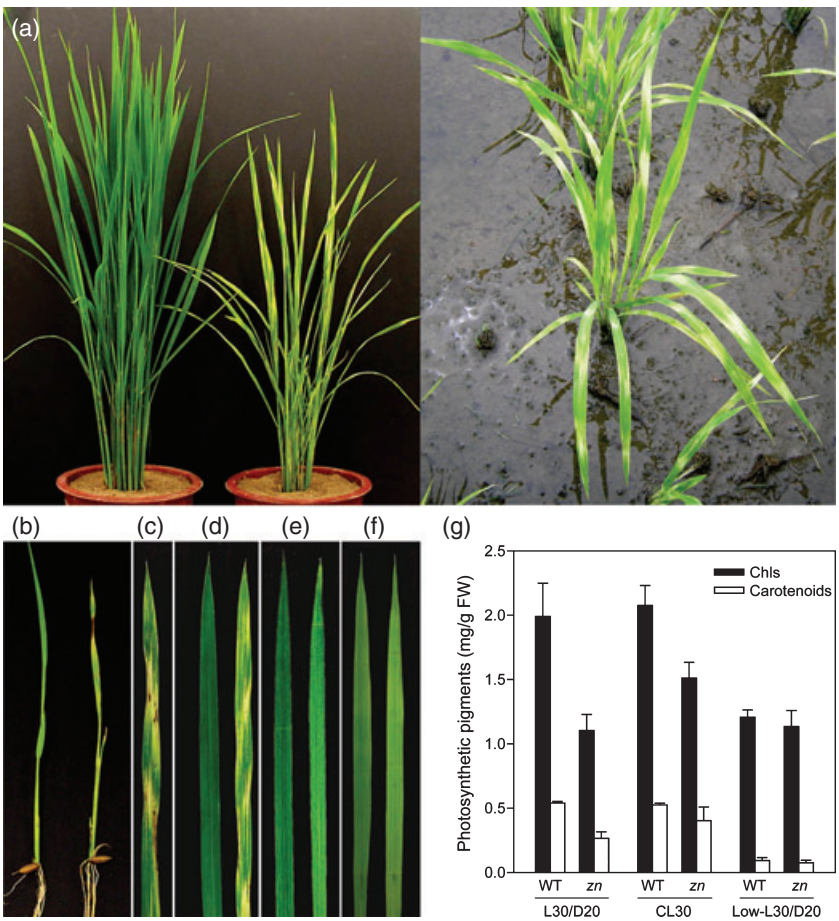

Figure 1. Phenotypic characteristics of the *zn* mutant.
(a, b) Phenotypes of 2-month-old plants (a) and 10-day-old seedlings (b) of a parental wild-type *japonica* cultivar 'Sinsunchalbyeo' (left) and mutant plants (right) grown in a paddy field.
(c) Necrosis (dark-brown spots) in the yellow leaf sectors of the mature leaves of mutant plants.
(d–f) Leaf blade phenotypes of the 1-month-old wild type (left) and mutant (right) plants. (d) Grown under 12-h light at 30°C and 12-h dark at 20°C (L30/D20). (e) Grown under constant light at 30°C (CL30). (f) Grown under L30/D20 with low light (20 μmol m^{-2} sec^{-1}; Low-L30/D20). All plants were grown in growth chambers. Rice plants were grown under cool-white fluorescent light (300 μmol m^{-2} sec^{-1}) unless otherwise stated.
(g) Chlorophyll (Chl) and carotenoid concentrations of the leaves of the wild type and mutant are shown in (d–f). Black and white boxes indicate total chlorophylls (Chls) and carotenoids, respectively. The mean and SD values were obtained from three replicates. Abbreviations: FW, fresh weight; WT, wild type.

of the leaf blades always develop from the early seedling stage (Figure 1b). This defective symptom becomes more severe as the leaves mature (Figure 1c).

Many previous reports showed that variegation/lesion mimic mutants are hypersensitive to light and/or temperature (Carol *et al.*, 1999; Kusumi *et al.*, 2000; Carol and Kuntz, 2001; Sugimoto *et al.*, 2004; Aluru *et al.*, 2006). We thus first examined the effects of light and temperature on the development of the mutant phenotype in growth chambers (Figure 1d–f). When the mutant plants were grown under normal conditions for wild-type rice plants (12-h white light, 300 μmol m^{-2} sec^{-1}, at 30°C and 12-h dark at 20°C; L30/D20), the concentrations of Chls and carotenoids in the mutant were about 50% of those of the wild type (Figure 1d,g, left). In contrast, the mutant phenotype had almost disappeared when they were grown under constant light at 30°C (CL30) (Figure 1e). However, the leaf color of the mutant was less green because the concentration of photosynthetic pigments was lower (Figure 1g, middle). Notably, not only did the mutant phenotype disappear completely under L30/D20 conditions with low-intensity light (20 μmol m^{-2} sec^{-1}; Low-L30/D20), but the pigment contents of the mutant were similar to that of the wild type (Figure 1f,g, right).

Microscopic analyses revealed that under permissive CL30 conditions, Chl-containing cells in the upper epidermal layers of the mutant leaves are almost normally distributed, despite the presence of a few Chl-free cells (Figure S1a,b). Under restrictive L30/D20 conditions, the *zn*-G sectors contain mostly Chl-containing cells, but Chl-free cells exist more frequently (Figure S1c). In the *zn*-Y sectors, most cells are Chl-free, but a few Chl-containing cells also exist, mainly around the small longitudinal veins (Figures S1d,e). We thus concluded that a mix of Chl-containing and Chl-free cells of different densities are present in the *zn*-G and *zn*-Y sectors (Figure S1f), although the mutant leaves display distinct transverse green/yellow stripe patterns.

The *zn* mutant phenotype is established before emergence from the leaf sheath

The effects of light and temperature on the expressivity of the *zn* mutation were investigated in more detail under permissive light conditions (300 μmol m^{-2} sec^{-1}) (Figure 2a–h). The overall results of this experiment demonstrate that the mutant phenotype is formed under diurnal fluctuations of either light/dark (12-h L/12-h D) (Figure 2b,c) or high/low temperatures (30°C/20°C) (Figure 2d). Only

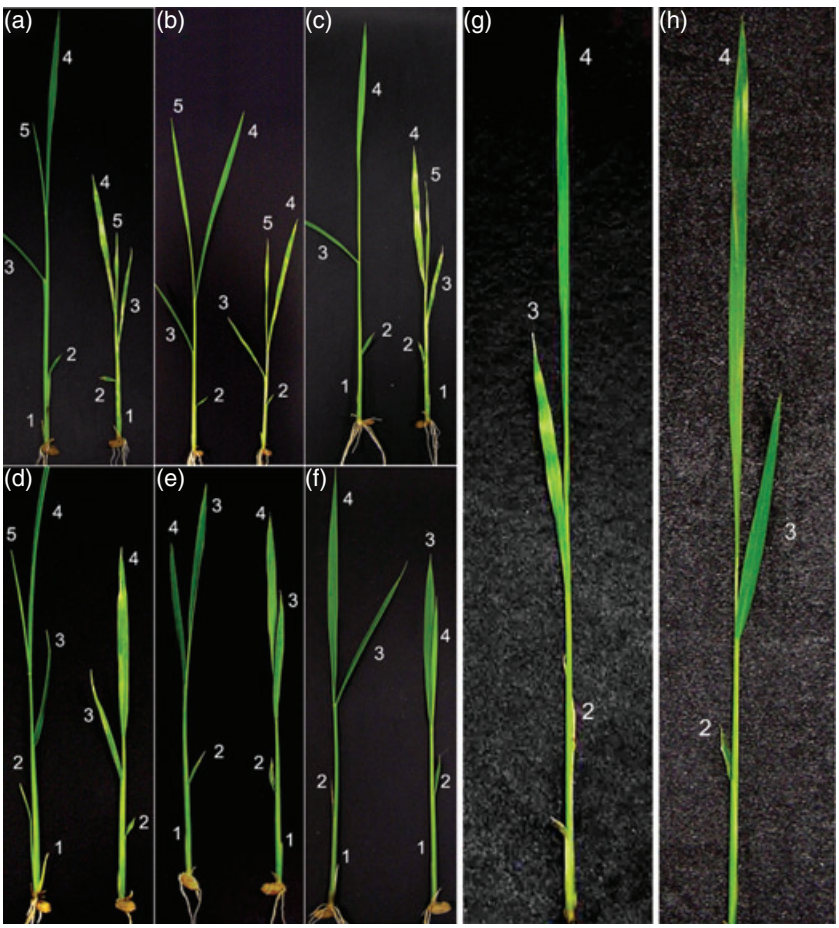

Figure 2. Effects of light and temperature on the development of the *zn* mutant phenotype.
(a–f) Phenotypes of the wild type (left) and mutant (right) grown in growth chambers: (a) under 12-h light at 30°C and 12-h dark at 20°C (L30/D20), (b) under 12-h light and 12-h dark at 20°C (C20L/D), (c) under under 12-h light and 12-h dark at 30°C (C30L/D), (d) under continuous light (CL) at 30°C for 12 h and 20°C for 12 h (CL30/20), (e) under CL at 20°C (CL20), and (f) under CL at 30°C (CL30).
(g, h) Phenotypic changes in the fourth leaf blade of mutant seedlings when shifted (g) from L30/D20 to CL30, or (h) from CL30 to L30/D20, conditions at half emergence of the third leaf blade from the leaf sheath. Plants were grown for 14 days after germination under white light (300 μmol m^{-2} sec^{-1}) in growth chambers. This experiment was repeated at least three times with the same results. Numbers 1–5 indicate the first to fifth leaf blades from the shoot base, respectively.

under constant light and temperature (CL20 and CL30) conditions do the mutant seedlings produce normal leaves, although these are a pale green (Figure 2e,f). Therefore, to discern the exact leaf developmental stage responsible for the onset of the mutant phenotype, we performed a shift experiment by transferring the mutant seedlings from restrictive L30/D20 to permissive CL30 conditions (Figure 2g), and *vice versa* (Figure 2h), when the third leaf had half-emerged from the leaf sheath. Shifting the mutant seedlings from restrictive to permissive conditions led to the production of a normal fourth leaf, whereas the third leaf maintained variegation (Figure 2g). Similarly, when they were transferred from permissive to restrictive conditions, the variegated fourth leaf emerged from the third leaf sheath, whereas the third leaf maintained a pale green color (Figure 2h), indicating the mutant phenotype is established before emergence of the leaf sheath under restrictive conditions, and is irreversible thereafter.

Chloroplast biogenesis is impaired in the Chl-free cells of the *zn* mutant

Under alternate high/low temperatures in complete darkness (CD30/20), the seedling phenotype of the *zn* mutant was indistinguishable from that of the wild type, with both exhibiting yellowish-brown leaf blades (data not shown). In addition, ultrastructural analysis revealed that shapes and internal structures of the etioplasts had no significant differences between them (Figure 3a,b), suggesting that the *zn* mutation does not affect the development of etioplasts. Chloroplast structures in the Chl-containing cells of a mutant grown under permissive CL30 (Figure 3d) and restrictive L30/D20 (Figure 3e) conditions appeared to be equivalent with those of the wild type (Figure 3c). Under restrictive conditions, however, the Chl-free cells had fewer and smaller defective plastids, with loose lamellar structures and several plastoglobuli (Figure 3f), which seemed to undergo irrevocable impairment in the middle of the synthesis of thylakoid membranes or during the assembly of thylakoid protein complexes.

Map-based cloning of *ZN* encoding a thylakoid-bound protein of unknown function

The *zn* locus has previously been mapped onto the classical genetic map of rice on the short arm of chromosome 6. To identify *ZN* using a map-based cloning method, 670 F_2 rice plants generated by a cross of the *zn* mutant (*japonica*) with

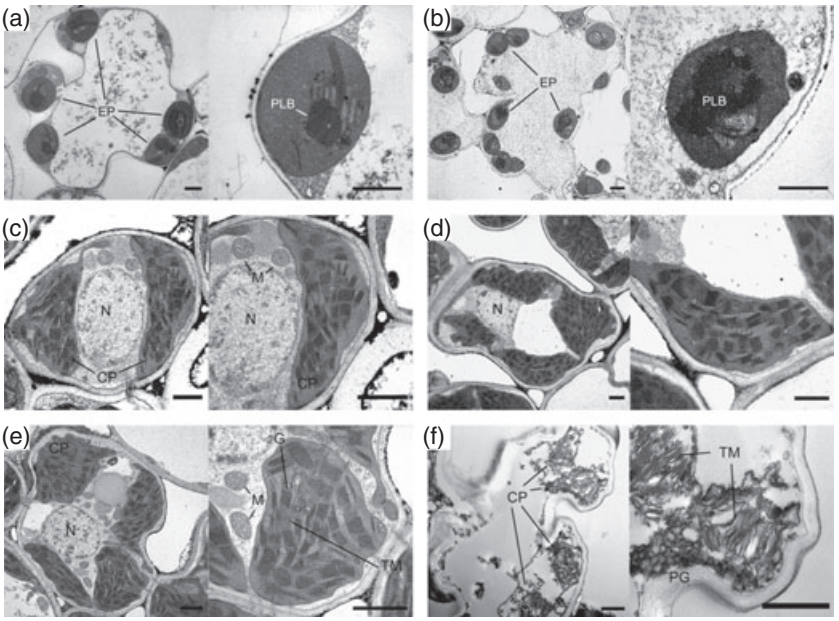

Figure 3. Transmission electron microscope (TEM) analysis of the *zn* mutant.
(a, b) Etioplasts in the mesophyll cells of dark-grown leaf tissues of (a) wild-type and (b) mutant seedlings. Germinating seeds were placed in complete darkness (CD), and leaf tissues of plants grown for 10 days under CD30/20 were then examined. Abbreviations: EP, etioplasts; PLB, prolamellar body. Scale bars: 1 μm.
(c–f) TEM samples were then obtained from (c) green leaves of wild-type plants grown in growth chambers under 12-h light at 30°C and 12-h dark at 20°C (L30/D20), (d) green leaves of the mutant plants grown under constant light at 30°C (CL30), and (e) green (*zn*-G) and (f) yellow (*zn*-Y) sectors of mutant plants grown under L30/D20. Abbreviations: CP, chloroplasts; G, grana; M, mitochondria; N, nucleus; PG, plastoglobuli; TM, thylakoid membranes. Scale bars: 1 μm.

Milyang23 (an *indica/japonica* hybrid cultivar) were first used to genetically map the *zn* locus. The analysis initially revealed that this gene was located within a 3.9-cM region between two simple sequence repeat (SSR) markers, RM8107 and RM8075, at the end region of the short arm of chromosome 6 (Figure 4a). By physical mapping, the *zn* locus was further delimited to within a 182-kb region between a sequence-tagged site marker, STS1 (AP001389, 82 kb), and an SSR marker, RM4784, in AP003564 (GenBank accession number) (Figure 4b). Because of the lack of polymorphic markers within this genomic region, we analyzed all of the genes identified by the Rice Genome Research Program (http://rgp.dna.affrc.go.jp). Twenty-two expressed and hypothetical genes (Figure 4c, top) were subsequently cloned by RT-PCR or genomic PCR. As a result, in AP002837, an expressed gene of unknown function (LOC_Os06g02580, GenBank accession number EU430513) comprising a 1292-bp-long region harboring two exons and one intron (exon 1–intron 1–exon 2) was identified in which the *zn* allele contains a single base transition from G to A at the start point of the 5′ splicing junction of intron 1 (Figure 4c, bottom), leading to a loss of function (Figure S2).

In the NCBI BLAST search, we found that a *ZN-like* gene (hereinafter referred to as *OsZNL*) exists on chromosome 3 (LOC_Os03g06090, EU430514) with a putative protein sequence that is highly homologous with ZN (hereafter referred to as OsZN) (Figure S3a). *OsZN* consists of a 1104-bp open reading frame (ORF) (Figure 4c, bottom) encoding 367 amino acids with a molecular mass of 37.7 kDa. OsZN harbors a chloroplast signal peptide at the N terminus, predicted by ChloroP and TargetP (Emanuelsson *et al.*, 1999, 2000), a bipartite thylakoid transit peptide [AXA(S/A/T/G)] that has a cleavage site for thylakoid lumen processing peptidase (Tissier *et al.*, 2002), and seven transmembrane domains (TMDs) (Figure 4d) predicted by ENSEMBLE (http://pongo.biocomp.unibo.it/pongo), as previously described (Eitinger *et al.*, 2005). The NCBI BLAST and the Gene Index Project databases (http://compbio.dfci.harvard.edu/tgi/cgi-bin/tgi/Blast/index.cgi) revealed that amino acid sequences of ZN homologs are highly conserved in all higher plants (Figure S3).

Expression analyses of *OsZN* showed that it is expressed only in the shoot organs, with the highest levels found in younger leaf tissues, but not in the roots (Figure 4e, top). *OsZN* mRNA is most abundant in the leaf tissues at the early developmental stage, and decreases thereafter (Figure 4e, middle). In contrast, the expression of *OsZNL* is the highest in the roots (Figure 4e, top), plausibly in the mitochondria, as predicted by TargetP (Figure S3a). In the wild-type rice seedlings, the levels of *OsZN* mRNA are approximately two-fold higher in the leaves of plants grown under continuous light (CL) than in those grown under complete darkness (CD), suggesting that *OsZN* is highly expressed by light at the transcriptional level (Figure 4e, bottom).

To complement the *zn* mutant phenotype, we constructed the recombinant binary vectors containing: (i) the genomic *ZN* fragment (*gZN*), along with 2 kb of the 5′ upstream region and 1 kb of the 3′ downstream region; and (ii) the *OsZN* ORF downstream of the cauliflower mosaic virus 35S promoter (*35S:OsZN*). These two recombinant plasmids were introduced independently into the calli of the *zn* seed embryos via *Agrobacterium*-mediated transformation. Fourteen *gZN* and nineteen *35S:OsZN* transformants produced normal green leaves, like the wild type, under restrictive L30/D20 conditions (Figure S4), indicating that the *zn* mutation is rescued by introducing the *OsZN* allele into the mutant.

OsZN is predicted to harbor a chloroplast-transit peptide at the N terminus. To confirm this prediction, we generated transgenic Arabidopsis plants containing *35S:OsZN-GFP* and *35S:GFP* (negative control). Confocal images of the protoplasts isolated from their rosette leaves revealed that OsZN localizes to the chloroplasts (Figure S5a). To further examine the intralocalization of ZN, the chloroplasts of transgenic Arabidopsis plants containing the *35S:AtZN1-GFP* (At2g16800; Figure S3b) were isolated, and their envelopes and thylakoids were then separated and immunoblotted, verifying that ZN is a thylakoid-bound protein (Figure S5b). Furthermore, ZN is preferentially associated with PSII among the photosynthetic complexes in the thylakoid membranes (Appendix S1; Figure S6).

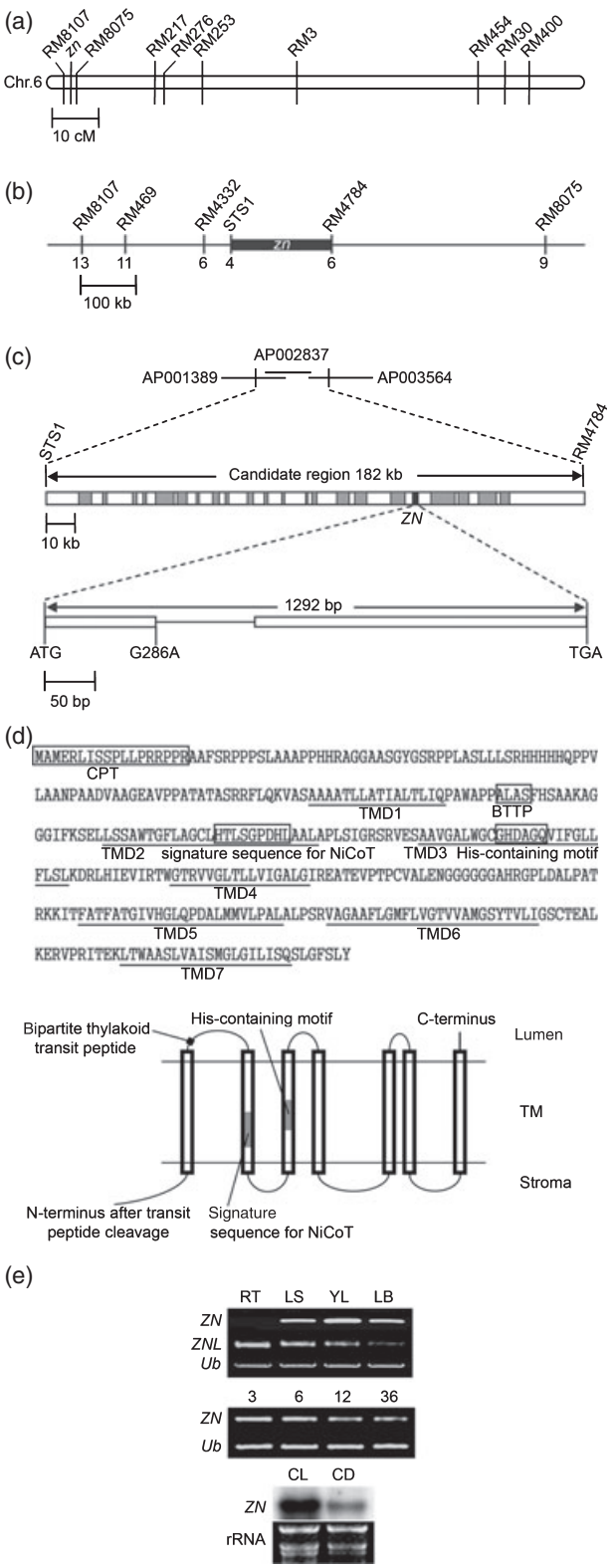

Figure 4. Map-based cloning and characterization of *ZN*.
(a) Genetic mapping of the *zn* locus. The *zn* locus was initially mapped to a 3.9-cM region between the simple sequence repeat (SSR) markers, RM8107 and RM8075, at the end of the short arm of chromosome 6. PCR-based SSR and sequence-tagged site (STS) marker primer information is listed in Table S1.
(b) Physical mapping of the *zn* locus. The *zn* locus was delimited to a 182.91-kb interval between STS1 and RM4784 using 22 F_2 recombinant individuals. Numbers indicate F_2 recombinants at the marker regions.
(c) Identification of Os*ZN* among 22 candidate genes. The genomic structure of *ZN* comprises two exons (white bars) and one intron (thin line). The point mutation yielding the *zn* mutant is a G → A transition at the start site of the 5′ splicing junction of intron 1.
(d) OsZN protein sequence. A predicted chloroplast targeting peptide (CPT), a bipartite thylakoid transit peptide (BTTP) and seven transmembrane domains (TMDs) are underlined. A topological model of OsZN integrated into the thylakoid membranes is shown in the lower panel, as depicted previously (Eitinger *et al.*, 2005).
(e) Expression profiles of *OsZN* and its homolog *OsZNL* in wild-type rice. (Top) Plants were cultivated for 15 days in growth chambers under 12-h light at 30°C and 12-h dark at 20°C (L30/D20). *OsZN* expression was then examined by semiquantitative RT-PCR. Abbreviations: LB, the expanded fourth leaf blade; LS, leaf sheath; RT, root; YL, the fourth leaf at emergence. (Middle) Plant samples were harvested from a paddy field. Total RNA samples from fourth leaf blades were extracted and used for semiquantitative RT-PCR. The numbers indicate days after leaf emergence from the sheath. The expression of *Ubiquitin* (*Ub*) was used as a loading control. (Bottom) Plants were grown for 10 days in growth chambers under continuous light with 30°C for 12 h and 20°C for 12 h (CL30/20) and continuous darkness with 30°C for 12 h and 20°C for 12 h (CD30/20) conditions.

The higher accumulation of ROS in the mutant leaves

To investigate whether necrotic lesions in the *zn*-Y sectors occur as a result of an excess accumulation of ROS, we examined the ROS levels in the mature leaves of the mutant (Figure 5a), particularly superoxide anion radicals and H_2O_2. Unexpectedly, we found that even under permissive CL30 conditions, the green mature leaves of the mutant accumulated more H_2O_2 (Figure 5b, left) and superoxide anion radicals (Figure 5c, left), by 3,3′-diaminobenzidine (DAB) and nitroblue tetrazolium (NBT) staining, respectively. Under restrictive L30/D20 conditions, it appeared that H_2O_2 accumulated at higher levels in the *zn*-Y sectors (Figure 5b, middle), whereas more superoxide anion radicals accumulated in the *zn*-G sectors (Figure 5c, middle). However, ROS accumulation was rarely observed in the pale-green leaves of mutants grown under Low-L30/D20 conditions (Figure 5b,c, right panels), or in the yellowish-brown etiolated

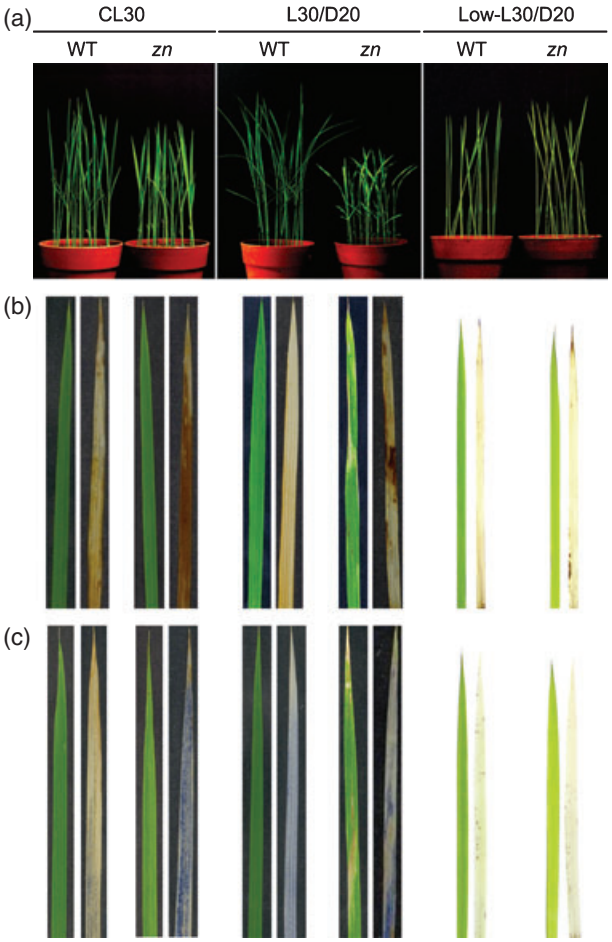

Figure 5. Reactive oxygen species (ROS) accumulation in the *zn* mutant.
(a) The wild-type and mutant plants were grown for 14 days after germination in growth chambers under constant light at 30°C (CL30), 12-h light at 30°C and 12-h dark at 20°C (L30/D20), and Low-L30/20 conditions as described in Figure 1.
(b, c) The fourth leaf blades of the wild-type and mutant plants in (a) were used for the detection of H_2O_2 (b) and superoxide anion radicals (c) by 3,3′-diaminobenzidine (DAB) and nitroblue tetrazolium (NBT) staining, respectively. These experiments were repeated more than three times with similar results.

seedlings grown under CD30/20 conditions (data not shown). We consistently observed a much higher accumulation of ROS in the etiolated mutant seedlings during greening (i.e. during the conversion from etioplasts to chloroplasts) under white light (300 μmol m^{-2} sec^{-1}) (data not shown). From these results, we became aware that newly developing plastids of the etiolated mutant leaves and defective plastids of the Chl-free cells in both *zn*-G and *zn*-Y sectors are the main source of light-inducible ROS.

The *zn* mutant is hypersensitive to photoinhibition

We found that the light-induced generation of ROS in the mutant leaves is not a result of defects in the Chl anabolic or catabolic pathway (Appendix S1; Figures S7 and S8). Moreover, the total activities of the ROS scavenging enzymes are actually enhanced in the mutant leaves (Appendix S1; Figure S9). As the scavengers superoxide dismutase (SOD) and ascorbate peroxidase (APX) do not interfere with singlet oxygen, it seems likely that the light-induced ROS production primarily enhances singlet oxygen concentration. We next examined the maximum quantum yield of PSII (variable fluorescence F_v/maximum fluorescence F_m) to assess the PSII function of the mutant. The F_v/F_m value of a healthy leaf is usually around 0.83 under normal growth conditions (Krause and Weis, 1991; Muthuchelian *et al.*, 2005). The F_v/F_m values of the *zn*-G and *zn*-Y sectors under restrictive L30/D20, and of the green leaves under permissive CL30, were all above 0.75 (Table 1). Furthermore, before or even after short-term photoinhibitory illumination, structures or functions of the photosynthetic apparatus were not impaired in the mutant (Appendix S1; Figures S10–13).These results indicate that the Chl-containing cells in both *zn*-G and *zn*-Y sectors (Figure S1) have chloroplasts of normal photosynthesis function, regardless of growth conditions.

We further tested whether the chloroplasts of the Chl-containing cells are more susceptible to photoinhibition. Under photoinhibitory illumination (1500 μmol m^{-2} sec^{-1}) for 2 h (Figure 6a), the F_v/F_m values of both the *zn*-G and *zn*-Y sectors of mutant grown under restrictive L30/D20 conditions rapidly dropped to 0.15 after 1 h of photoinhibitory irradiation, but it was reduced to only 0.28 in the wild type. Even under permissive CL30 conditions, the mutant was also more sensitive to photoinhibition than the wild type (Figure 6b), indicating that the PSII activity is hypersensitive to

Table 1 Chlorophyll fluorescence parameters in the wild-type and mutant plants grown under restrictive, 12-h light at 30°C and 12-h dark at 20°C (L30/D20), and permissive, constant light at 30°C (CL30), conditions

	L30/D20			CL30	
Parameter	Wild type	*zn*-G	*zn*-Y	Wild type	*zn*
F_0	0.18 ± 0.04	0.12 ± 0.02	0.05 ± 0.02	0.23 ± 0.02	0.16 ± 0.01
F_m	1.04 ± 0.20	0.54 ± 0.12	0.21 ± 0.10	1.12 ± 0.02	0.82 ± 0.02
F_v/F_m	0.82 ± 0.01	0.78 ± 0.01	0.75 ± 0.02	0.80 ± 0.02	0.80 ± 0.01

The F_0 and F_m values were measured in fully matured third leaf blades of 1-month-old plants raised in growth chambers, and F_v was caluclated using $F_v = F_m - F_0$. Mean and SD values were obtained from five replicates. *zn*-G and *zn*-Y represent the green and yellow sectors of the mutant, respectively.

photoinhibition, independent of growth conditions. To distinguish whether this hypersensitivity of normal chloroplasts in the Chl-containing cells of the mutant is caused by accelerated damage to PSII or impaired repair of photodamaged PSII, the plants were illuminated in the presence of lincomycin (an inhibitor of chloroplast protein synthesis), which blocks PSII repair. Under both growth conditions, the F_v/F_m values of both the wild type and the mutant rapidly decreased (by approximately 88%) at the same rate during a 2-h period of photoinhibitory illumination (Figure 6c,d), suggesting that the rate of PSII inactivation does not differ between the wild type and the mutant. Interestingly, in the absence of lincomycin (–LN), the decrease of the F_v/F_m values of the mutant leaves proceeded with the same rapid kinetics as the lincomycin-treated (+LN) mutant leaves under both growth conditions (Figure 6a–d). This finding suggests that regardless of growth conditions the hypersensitivity of the mutant to high light stress is caused by preferential impairment of PSII repair, rather than by a greater degree of inactivation of PSII.

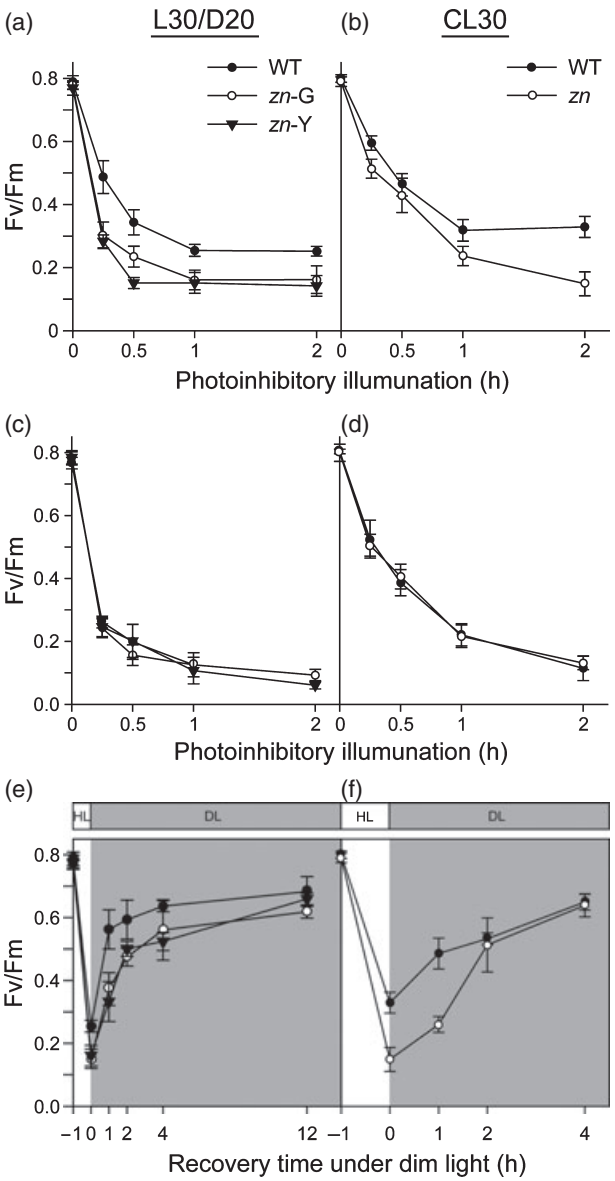

Figure 6. Photoinhibition of photosystem II (PSII) and subsequent recovery kinetics in the *zn* mutant. Leaf blades were detached from the plants grown under the restrictive 12-h light at 30°C and 12-h dark at 20°C (L30/D20) (a, c, e) and permissive constant light at 30°C (CL30) (b, d, f) conditions in growth chambers, and the F_v/F_m values were measured under photoinhibitory illumination at 1500 μmol m^{-2} sec^{-1} for 2 h in the absence (a, b) or presence (c, d) of lincomycin.
(e, f) The wild-type and mutant leaves were then exposed to photoinhibitory illumination at 1500 μmol m^{-2} sec^{-1} for 1 h, and subsequent recovery was followed by exposure to dim light at 20 μmol m^{-2} sec^{-1} at room temperature. A time of –1 h represents overnight dark adaptation prior to high light treatment. A time of 0 h represents the end of the 1-h high light treatment, and 1, 2, 4 and/or 12 h represent subsequent recovery periods under dim light at 20 μmol m^{-2} sec^{-1} at room temperature. Means and SD values were obtained from five replicates. White and grey areas represent photoinhibitory illumination and recovery periods, respectively.

The wild type and the mutant were next treated by photoinhibitory illumination (1500 μmol m^{-2} sec^{-1}) for 1 h and then placed under dim light (20 μmol m^{-2} sec^{-1}) for PSII recovery, which is a requirement for the synthesis of new D1 during the reassembly of the PSII reaction center. We found that the recovery of PSII function in the wild-type leaves was faster than that of the mutant leaves at the start of dim-light treatment, independent of the growth conditions (Figure 6e,f). However, the F_v/F_m values of the mutant grown under both L30/D20 and CL30 conditions reached almost the wild-type levels after 12 and 4 h of recovery under dim light, respectively, suggesting that the hypersensitivity to photoinhibition may result from the attenuation of the PSII repair process in the functional chloroplasts of Chl-containing cells.

The protease-mediated degradation of damaged D1 during PSII repair is not impaired in the *zn* mutant

The D1 protein of PSII is easily damaged by excess light, and damaged D1 must be degraded rapidly and replaced by newly synthesized D1 to reactivate PSII function. Hence, we examined whether the inefficient repair cycle of PSII is caused by a defect in the D1 degradation steps, akin to the *yellow variegated* (*var*) mutants of Arabidopsis (Chen *et al.*, 2000; Bailey *et al.*, 2002; Sakamoto *et al.*, 2002). Immunoblot analyses were thus performed using an antibody specific to a lumen-exposed C-terminal part of D1 (D1C) (Figure 7). When the pale green leaves of plants grown under permissive CL30 conditions were subjected to photoinhibitory illumination (1500 μmol m^{-2} sec^{-1}), total concentrations of the 23 and 16-kDa fragments of D1 were considerably higher in the mutant leaves (Figure 7a), indicating a greater degree of inactivation of PSII by high light stress (Figure 6b) (Miyao, 1994). However, in the presence of lincomycin (+LN), the levels of degraded D1 fragments in the mutant did not significantly differ from those in the wild type (Figure 7b). We also obtained similar results when the *zn*-G sectors of

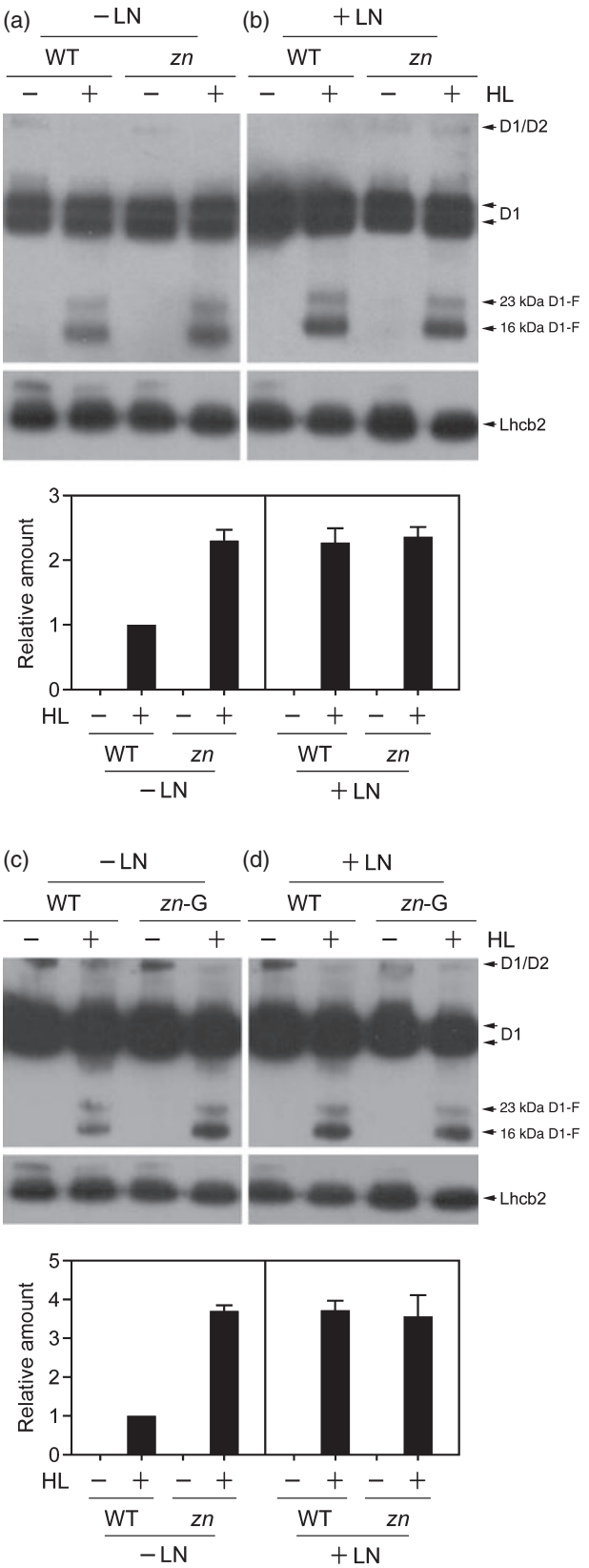

mutants grown under restrictive L30/D20 conditions were subjected to photoinhibitory illumination (Figure 7c,d). These results indicate that the protease-mediated degradation of photodamaged D1 is not altered by the *zn* mutation. Thus, we concluded that a slow recovery of the PSII activity from photoinhibition (Figure 6e,f) is mainly the result of delayed synthesis of new D1 during PSII repair.

DISCUSSION

Here, we report the phenotypic characteristics of the rice *zn* mutant, and the positional cloning of *ZN*, which encodes a thylakoid-bound protein of unknown function. Given that the mutant phenotype is closely associated with the biogenesis of chloroplasts that have been unequally damaged by incidental light after a period of darkness (Figures 1, 2, and S1), it seems intuitive that normal development of the etioplasts in the dark would occur in the mutant leaves (Figure 3a,b). Both the Chl-containing cells having normal chloroplasts, and Chl-free cells containing defective chloroplasts are mixed together at different densities (Figures 3c–f and S1), leading to the formation of transverse green/yellow stripes (*zn*-G and *zn*-Y) in a monocot plant (rice) and sporadic green/yellow sectors in a dicot plant (*Nicotiana benthamiana*; Appendix S1; Figure S14). The onset of this variegation seems to be confined to the early stages of leaf development, i.e. prior to emergence from the leaf sheath under restrictive conditions (Figure 2). *OsZN* is constitutively expressed at low levels in the etiolated seedlings, and is highly transcribed in the de-etiolated seedlings, but not in the roots (Figure 4e, top). In addition, *OsZN* transcripts are highly transcribed during early leaf development, and its expression decreases thereafter. Thus, we propose that ZN is a critical component for protecting the developing chloroplasts of newly dividing leaf cells from photodamage under normal growth conditions, i.e. alternate light/dark and day/night temperatures. Hypersensitivity to alternate high/low temperatures under constant light (Figure 2d) remains to be determined.

The ZN homologs of higher plants are mainly predicted to localize in the chloroplasts (Figure S3). Interestingly, they have a similar signature sequence (HTLSGPDHL) in TMD-II,

Figure 7. Immunoblot analysis of D1 and its degraded fragments from photoinhibition. The wild-type and mutant plants were grown for 14 days in growth chambers under conditions of constant light at 30°C (CL30) (a, b) and 12-h light at 30°C and 12-h dark at 20°C (L30/D20) (c, d), as described in Figure 1. The leaf blades were then detached and exposed to 1500 μmol m^{-2} sec^{-1} (+HL) for 1 h in the absence (a, c) or presence (b, d) of lincomycin (LN). Thylakoid membranes were then isolated and 2 μg of chlorophyll (Chl) was loaded into each lane. Degraded D1 fragments were detected with D1-specific antibodies both before and after photoinhibitory illumination. After D1 detection, the LHCII levels were immunoblotted with an anti-Lhcb2 antibody as an internal loading control. Relative quantities of 16-kDa D1-F were divided by the values of the wild type (−LN/HL). Means and SDs are obtained from three replicates. D1, 32-kDa D1; D1/D2, 65-kDa heterodimer of D1 and D2; D1-F, degraded D1 fragment.

and a His-containing motif (GHDAGQ) in TMD-III, to a high-affinity nickel/cobalt transporter (NiCoT), one of the secondary metal transporter families in bacteria and fungi (Eitinger *et al.*, 2005). Except for the topological similarity, amino acid sequences of ZN homologs are quite different from those of bacterial NiCoTs, and have no His-repeating motifs (up to 14 His residues) in the stromal loops between TMD-IV and TMD-V, which seems to play an important role in cellular Ni affinity, compared with UreH in the bacterial urease operons, and SodT in the Ni-dependent SOD operons in many marine cyanobacteria (Eitinger *et al.*, 2005). Urease is a unique Ni-binding enzyme among metalloenzymes of plants, and its cytoplasmic and intercellular localization has been identified in jack bean (*Canavalia* spp.) (Murray and Knox, 1977). However, the urease activity is not altered in the mutant leaves (Figure S15), indicating that the *zn* mutation is irrelevant to the urease activity. Furthermore, using an inductive coupled plasma spectrum (data not shown), we could not obtain any evidence of alteration in the concentrations of several metal ions (Ni, Co, Zn, Mg, Mn, Cu or Fe) of the leaves, or purified chloroplasts, between the wild type and the *zn* mutant, or between the wild type and the OsZN- or AtZN1-overexpressed transgenic plants of Arabidopsis (Figure S5b). These negative results suggest that ZN may not act as a secondary metal transporter, although this should be further verified.

Unlike albinism, leaf variegation is a nonlethal trait, and is formed by sectors that contain either normally appearing chloroplasts or abnormally arrested/defective plastids (Sakamoto, 2003; Aluru *et al.*, 2006, 2009). In this study, a fundamental question is which principal mechanism leads to variegation in the same leaf tissues of the mutant. We consistently observed that during greening (i.e. during the conversion from etioplasts to chloroplasts) of dark-grown etiolated seedlings under permissive conditions (300 μmol m^{-2} sec^{-1}), more ROS accumulated in the already developed leaf blades of the mutant compared with those of the wild type (data not shown). Based on the shapes and internal structures of defective plastids of the Chl-free cells (Figure S1d,f), it is evident that an impediment of chloroplast biogenesis occurs during the assembly of thylakoid protein complexes, possibly during the biogenesis of PSII, as ZN is preferentially associated with the PSII complex in the thylakoid membranes (Figure S6). It suggests that in the absence of ZN, newly differentiating chloroplasts are highly susceptible to damage from incidental light through an as-yet undefined mechanism, and the impaired plastids lead to the formation of Chl-free cells (Figure 3f). Our shift experiments strongly support this notion that the fate of chloroplasts of photosynthetic cells is irreversibly determined at this early stage of chloroplast biogenesis (Figure 2g,h). Based on this scenario, it is possible to explain the presence of Chl-containing cells in the mutant leaves: at a critical stage of thylakoid complex formation, some developing chloroplasts escape from photodamage during the night period, or by chance under low-intensity light at dawn, and subsequently differentiate into the chloroplasts of normal shapes and functions (Figures 3d and S1F). In the Chl-containing cells, however, ROS may also be produced from the chloroplasts under restrictive conditions, but those levels are not critical enough to induce oxidative damage because the ROS scavenging activities have also been greatly elevated in the mutant leaves (Figure S9).

Prolonged oxidative conditions in the defective plastids of Chl-free cells appear to be the main source of ROS under excess light (Figure 5). We observed that under a medium intensity (100 μmol m^{-2} sec^{-1}) of white light, the zebra phenotype was clearly developed, but necrosis in the *zn*-Y sectors never occurred under restrictive L30/D20 conditions (data not shown), indicating that the phenotypic severity and ROS levels from the Chl-free cells are directly correlated with an increase in light intensity. Furthermore, we could not find any abnormalities in chlorophyll biosynthesis and catabolism, total cellular activities of SOD and APX for ROS detoxification, F_v/F_m as a measure of the maximum PSII quantum yield, or structures and functions of the photosynthetic complexes in the functional chloroplasts of Chl-containing cells (Figures S7–13; Table 1). We only found that its PSII activity is hypersensitive to photoinhibition (Figure 6a,c) because of a slow recovery of the PSII activity under dim light, regardless of growth conditions (Figure 6e,f). The protease-mediated degradation of damaged D1 is not impaired (Figure 7), strongly suggesting that the de novo synthesis of D1 is not fully active in the PSII repair cycle of the mutant. It should be noted that ROS suppress PSII repair at the translational level of new D1 synthesis (Nishiyama *et al.*, 2001; Murata *et al.*, 2007; Takahashi and Murata, 2008). In addition, ROS has a high diffusion rate, and specific aquaporins facilitate its diffusion across the biological membranes (Bienert *et al.*, 2007). We showed that the leaf phenotype and pigment concentrations of the mutant were almost identical with those of the wild type under Low-L30/D20 conditions (Figure 1f,g), and that ROS accumulation was barely detectable in the pale green leaves of the mutant (Figure 5, right panels) because the defective Chl-free cells were hardly found (data not shown). In this respect, it is highly possible that although the Chl-free cells are unable to green normally, and the assembly of thylakoid membrane components is irreversibly disturbed, the trace levels of Chls may still be synthesized in the absence of membrane assembly, because tetrapyrrole synthesis in the *zn* mutant seems to operate as indicated by the 5-aminolevulinate (ALA) feeding experiment and HPLC analysis of pigments (Figures S7 and S8). They may act as photosensitizers that can generate singlet oxygen under high-intensity light. Thus, during photoinhibitory irradiation, the elevated levels of singlet oxygen generated from the Chl-free cells may negatively affect the de novo

synthesis of D1 in normal chloroplasts in the Chl-containing cells, resulting in hypersensitivity to photoinhibition. In other words, the inefficient repair cycle of PSII in the mutant leaves mainly results from elevated levels of ROS under high-intensity light. Further identification of the genes responsible for other *zebra* mutations of rice is ongoing in our laboratory, and will enable us to provide more insights into the molecular function of ZN, as well as new components involved in the photoprotection of developing chloroplasts during early leaf development in higher plants.

EXPERIMENTAL PROCEDURES

Plant materials and growth conditions

The *zn* mutation was induced by applying a chemical mutagen *N*-methyl-*N*-nitrosourea (MNU) to the fertilized egg cells of a Korean glutinous *japonica* rice cultivar 'Sinsunchalbyeo', as previously described (Kim *et al.*, 1991). The wild-type 'Sinsunchalbyeo' and the *zn* mutant plants were cultivated in a paddy field or in growth chambers. The chamber conditions were as follows: alternate 12-h light with low intensity (20 μmol m^{-2} sec^{-1}) at 30°C and 12-h dark at 20°C (Low-L30/D20); alternate 12-h light (300 μmol m^{-2} sec^{-1}) at 30°C and 12-h dark at 20°C (L30/D20); alternate 12-h light and 12-h dark at a constant 20°C (C20L/D) or 30°C (C30L/D); continuous light with 30°C for 12 h and 20°C for 12 h (CL30/20); continuous light at 20°C (CL20) or 30°C (CL30).

Measurement of photosynthetic pigments

Pigments were extracted from equal fresh weights of leaf tissues with 80% ice-cold acetone. The concentrations of Chls and carotenoids were determined with a UV/VIS spectrophotometer according to Lichtenthaler's (1987).

Confocal and transmission electron microscopy (TEM) analyses

For microscopic analysis, a confocal laser scanning microscope (Zeiss, http://www.zeiss.com) and a transmission electron microscope (JEM-1010; JEOL, http://www.jeol.com) were used, as previously described (Park *et al.*, 2007).

Histochemical detection of superoxide anion radicals and hydrogen peroxide

Histochemical assays for ROS accumulation were conducted as previously described (Fryer *et al.*, 2002; Kariola *et al.*, 2005; Mahalingam *et al.*, 2006; Lin *et al.*, 2009). Briefly, for the determination of superoxide anion radicals, leaf samples were immersed in 6 mM NBT solution containing 50 mM HEPES buffer (pH 7.5) for 2 h in the dark. For H_2O_2 detection, detached leaves were immersed in 5 mM DAB solution containing 10 mM 2-(*N*-morpholine)-ethanesulphonic acid (MES; pH 3.8) for 8 h in darkness.

Genetic and physical mapping

A mapping population of 670 F_2 individuals was produced by crossing a *japonica*-type *zn* mutant and a tongil-type cultivar, Milyang23, which is derived from an *indica* × *japonica* hybridization, and has a genetic make-up that is close to that of *indica*. To confirm the chromosomal localization of the *zn* locus, we had previously performed small-scale mapping using forty *zn* homozygous F_2 plants and nine SSR markers distributed on chromosome 6 (this information is available in GRAMENE; http://www.gramene.org). Three SSR markers and one STS marker (STS1) were used for physical mapping.

Measurement of Chl fluorescence and photoinhibitory illumination

The leaves were detached from 15-day-old rice plants and cultivated in growth chambers under L30/D20 or CL30 conditions. Prior to dark adaptation, leaf segments were prepared in water to protect against severe wounding, and were then floated on water (control) or immersed in 3 mM lincomycin using a single layer of Kimwipes. The segments were then kept in the dark at 20°C overnight to enable lincomycin infiltration. The minimum (F_0) and maximum (F_m) Chl fluorescence of PSII was then measured using a portable fluorometer (PAM-2000; Walz, http://www.walz.com) at room temperature (22–24°C). Next, the leaf segments were dark-adapted for 30 min prior to fluorescence measurements at room temperature. The maximum quantum yield of PSII photochemistry, F_v/F_m, was calculated as $F_v/F_m = (F_m - F_0)/F_m$ (Genty *et al.*, 1989). All measurements were performed in a dark room under stable ambient conditions. *In vivo* photoinhibition was induced by illumination with white light (1500 μmol m^{-2} sec^{-1}) from a metal halide lamp to induce PSII photodamage with or without lincomycin, and a 15-cm-deep water bath was placed under the lamp, and was cooled with an air conditioner to prevent overheating. Photoinhibition was assessed by measuring the F_v/F_m values before and after high light treatments using a portable fluorometer. A saturating light pulse (3000 μmol m^{-2} sec^{-1} for 800 msec) was used to measure F_m. After photoinhibition, leaf samples were placed under dim white light (20 μmol m^{-2} sec^{-1}) to induce de novo synthesis for the repair of damaged PSII for the indicated time periods.

Preparation of thylakoids and immunoblotting analysis

The thylakoid membrane fractions from leaf tissues were prepared and Chl concentration was measured as described previously (Porra *et al.*, 1989). The levels of D1 protein and its degradation were detected as described by Miyao (1994) using a D1C-specific antibody against the C terminal of the D1 protein generously donated by M. Miyao (NIAR, Japan). An anti-Lhcb2 antibody (AgriSera, http://www.agrisera.com) was used as a loading control.

ACKNOWLEDGEMENTS

We thank Dr S.P. Dinesh-Kumar (Yale University, USA) for the donation of TRV plasmids for the virus-induced gene silencing experiments and Dr Seung-Gon Wi (Chonnam National University, Korea) for his technical assistance. This research was supported by a grant (CG3131) from the Crop Functional Genomics Center of the 21C Frontier R&D Program, and by an Agricultural Plant Stress Research Center grant (R11-2001-092-05003-0) from the KOSEF, Korea.

SUPPORTING INFORMATION

Additional Supporting Information may be found in the online version of this article:

Figure S1. Microscopic analyses of chloroplasts in the *zn* mutant.

Figure S2. Abnormal splicing variants from the primary transcripts of *OsZN* in the *zn* mutant.

Figure S3. CLUSTALW alignments of ZN homologs in higher plants.

Figure S4. Complementation of the *zn* mutation.

Figure S5. ZN is localized in the thylakoid membranes of chloroplasts.

Figure S6. ZN is associated with photosystem II (PSII) among the photosynthetic complexes.

Figure S7. Protochlorophyllide concentrations in the ALA-fed seedlings.
Figure S8. HPLC analysis of the chlorophyll and carotenoid contents in the *zn* mutant.
Figure S9. Total superoxide dismutase (SOD) and ascorbate peroxidase (APX) activities in the *zn* mutant.
Figure S10. Separation of thylakoid protein complexes and supercomplexes by blue native polyacrylamide gel electrophoresis (BN-PAGE).
Figure S11. Immunoblot analysis of major thylakoid proteins in the *zn* mutant.
Figure S12. Electron transport rate in the *zn* mutant.
Figure S13. Non-photochemical and photochemical quenching in the *zn* mutant.
Figure S14. Virus-induced gene silencing (VIGS) of a *ZN* homolog in *Nicotiana benthamiana*.
Figure S15. Urease activity in the *zn* mutant.
Table S1. Primer information used in this study.
Appendix S1. Supplementary results, experimental procedures and references.
Please note: As a service to our authors and readers, this journal provides supporting information supplied by the authors. Such materials are peer-reviewed and may be re-organized for online delivery, but are not copy-edited or typeset. Technical support issues arising from supporting information (other than missing files) should be addressed to the authors.

REFERENCES

Ahmad, P., Sarwat, M. and Sharma, S. (2008) Reactive oxygen species, antioxidents and signaling in plants. *J. Plant Biol.* **51**, 167–173.
Aluru, M.R., Bae, H., Wu, D. and Rodermel, S.R. (2001) The Arabidopsis *immutans* mutation affects plastid differentiation and the morphogenesis of white and green sectors in variegated plants. *Plant Physiol.* **127**, 67–77.
Aluru, M.R., Yu, F., Fu, A. and Rodermel, S. (2006) *Arabidopsis* variegation mutants: new insights into chloroplast biogenesis. *J. Exp. Bot.* **57**, 1871–1881.
Aluru, M.R., Zola, J., Foudree, A. and Rodermel, S. (2009) Chloroplast photooxidation-induced transcriptome reprogramming in Arabidopsis *immutans* white leaf sectors. *Plant Physiol.* **150**, 904–923.
Apel, K. and Hirt, H. (2004) Reactive oxygen species: metabolism, oxidative stress, and signal transduction. *Annu. Rev. Plant Biol.* **55**, 373–399.
Aro, E.M., Virgin, I. and Andersson, B. (1993) Photoinhibition of photosystem II. Inactivation, protein damage and turnover. *Biochim. Biophys. Acta*, **1143**, 113–134.
Bailey, S., Thompson, E., Nixon, P.J., Horton, P., Mullineaux, C.W., Robinson, C. and Mann, N.H. (2002) A critical role for the Var2 FtsH homologue of *Arabidopsis thaliana* in the photosystem II repair cycle in vivo. *J. Biol. Chem.* **277**, 2006–2011.
Bienert, G.P., Møller, A.L., Kristiansen, K.A., Schulz, A., Møller, I.M., Schjoerring, J.K. and Jahn, T.P. (2007) Specific aquaporins facilitate the diffusion of hydrogen peroxide across membranes. *J. Biol. Chem.* **282**, 1183–1192.
Carol, P. and Kuntz, M. (2001) A plastid terminal oxidase comes to light: implications for carotenoid biosynthesis and chlororespiration. *Trends Plant Sci.* **6**, 31–36.
Carol, P., Stevenson, D., Bisanz, C., Breitenbach, J., Sandmann, G., Mache, R., Coupland, G. and Kuntz, M. (1999) Mutations in the *Arabidopsis* gene *IMMUTANS* cause a variegated phenotype by inactivating a chloroplast terminal oxidase associated with phytoene desaturation. *Plant Cell*, **11**, 57–68.
Chen, M., Choi, Y., Voytas, D.F. and Rodermel, S.R. (2000) Mutations in the *Arabidopsis VAR2* locus cause leaf variegation due to the loss of a chloroplast FtsH protease. *Plant J.* **22**, 303–313.
Eitinger, T., Suhr, J., Moore, L. and Smith, J.A. (2005) Secondary transporters for nickel and cobalt ions: theme and variations. *Biometals*, **18**, 399–405.
Emanuelsson, O., Nielsen, H. and von Heijne, G. (1999) ChloroP, a neural network-based method for predicting chloroplast transit peptides and their cleavage sites. *Protein Sci.* **8**, 978–984.
Emanuelsson, O., Nielsen, H., Brunak, S. and von Heijne, G. (2000) Predicting subcellular localization of proteins based on their N-terminal amino acid sequence. *J. Mol. Biol.* **300**, 1005–1016.
Fryer, M.J., Oxborough, K., Mullineaux, P.M. and Baker, N.R. (2002) Imaging of photo-oxidative stress responses in leaves. *J. Exp. Bot.* **53**, 1249–1254.
Genty, B., Briantais, J.-M. and Baker, N.R. (1989) The relationship between the quantum yield of photosynthetic electron transport and quenching of chlorophyll fluorescence. *Biochim. Biophys. Acta*, **990**, 87–92.
Hansson, M., Gough, S.P., Kannangara, C.G. and von Wettstein, D. (1997) Analysis of RNA and enzymes of potential importance for regulation of 5-aminolevulinic acid synthesis in the protochlorophyllide accumulating barley mutant *tigrina*-D (12). *Plant Physiol. Biochem.* **35**, 827–836.
Kariola, T., Brader, G., Li, J. and Palva, E.T. (2005) Chlorophyllase 1, a damage control enzyme, affects the balance between defense pathways in plants. *Plant Cell*, **17**, 282–294.
Kim, K.-H., Heu, M.-H., Park, S.-Z. and Koh, H.-J. (1991) New mutants for endosperm and embryo characters in rice. *Korean J. Crop Sci.* **36**, 197–203.
Kojo, K., Yaeno, T., Kusumi, K., Matsumura, H., Fujisawa, S., Terauchi, R. and Iba, K. (2006) Regulatory mechanisms of ROI generation are affected by rice *spl* mutations. *Plant Cell Physiol.* **47**, 1035–1044.
Krause, G.H. and Weis, E. (1991) Chlorophyll fluorescence and photosynthesis: the basics. *Annu. Rev. Plant Physiol. Plant Mol. Biol.* **42**, 313–349.
Kusumi, K., Komori, H., Satoh, H. and Iba, K. (2000) Characterization of a *zebra* mutant of rice with increased susceptibility to light stress. *Plant Cell Physiol.* **41**, 158–164.
Lichtenthaler, H.K. (1987) Chlorophylls and carotenoids: pigments of photosynthetic biomembranes. *Methods Enzymol.* **148**, 351–382.
Lin, Z.-F., Liu, N., Lin, G.-Z. and Peng, C.-L. (2009) In situ localisation of superoxide generated in leaves of *Alocasia macrorrhiza* (L.) Shott under various stresses. *J. Plant Biol.* **52**, 340–347.
Mahalingam, R., Jambunathan, N., Gunjan, S.K., Faustin, E., Weng, H. and Ayoubi, P. (2006) Analysis of oxidative signaling induced by ozone in *Arabidopsis thaliana*. *Plant Cell Environ.* **29**, 357–1371.
Meskauskiene, R., Nater, M., Goslings, D., Kessler, F., op den Camp, R. and Apel, K. (2001) FLU: a negative regulator of chlorophyll biosynthesis in *Arabidopsis thaliana*. *Proc. Natl Acad. Sci. USA*, **98**, 12826–12831.
Miura, E., Kato, Y., Matsushima, R., Albrecht, V., Laalami, S. and Sakamoto, W. (2007) The balance between protein synthesis and degradation in chloroplasts determines leaf variegation in *Arabidopsis yellow variegated* Mutants. *Plant Cell*, **19**, 1313–1328.
Miyao, M. (1994) Involvement of active oxygen species in degradation of the D1 protein under strong illumination in isolated subcomplexes of photosystem II. *Biochemistry*, **33**, 9722–9730.
Murata, N., Takahashi, S., Nishiyama, Y. and Allakhverdiev, S.I. (2007) Photoinhibition of photosystem II under environmental stress. *Biochim. Biophys. Acta*, **1767**, 414–421.
Murray, D.R. and Knox, R.B. (1977) Immunofluorescent localization of urease in the cotyledons of jack bean, *Canavalia ensiformis*. *J. Cell Sci.* **26**, 9–18.
Muthuchelian, K., Porta, N.L., Bertamini, M. and Nedunchezhian, N. (2005) Cypress canker induced inhibition of photosynthesis in field growth cypress (*Cupressus sempervirens* L.) needles. *Physiol. Mol. Plant Pathol.* **67**, 33–39.
Nishiyama, Y., Yamamoto, H., Allakhverdiev, S.I., Inaba, M., Yokota, A. and Murata, N. (2001) Oxidative stress inhibits the repair of photodamage to the photosynthetic machinery. *EMBO J.* **20**, 5587–5594.
Overmyer, K., Brosche, M. and Kangasjarvi, J. (2003) Reactive oxygen species and hormonal control of cell death. *Trends Plant Sci.* **8**, 335–342.
Park, S.-Y., Yu, J.-W., Park, J.-S. *et al.* (2007) The senescence-induced staygreen protein regulates chlorophyll degradation. *Plant Cell*, **19**, 1649–1664.
Porra, R.J., Thompson, W.A. and Kriedemann, P.E. (1989) Determination of accurate extinction coefficients and simultaneous equations for assaying chlorophyll a and b with four different solvents: verification of the concentration of chlorophyll by atomic absorption spectroscopy. *Biochim. Biophys. Acta*, **975**, 384–394.
Pružinská, A., Tanner, G., Anders, I., Roca, M. and Hörtensteiner, S. (2003) Chlorophyll breakdown: pheophorbide *a* oxygenase is a Rieske-type iron-sulfur protein, encoded by the *accelerated cell death 1* gene. *Proc. Natl Acad. Sci. USA*, **100**, 15259–15264.

Pružinská, A., Anders, I., Aubry, S., Schenk, N., Tapernoux-Lüthi, E., Müller, T., Kräutler, B. and Hörtensteiner, S. (2007) In vivo participation of red chlorophyll catabolite reductase in chlorophyll breakdown. *Plant Cell*, **19**, 369–387.

Sakamoto, W. (2003) Leaf-variegated mutations and their responsible genes in *Arabidopsis thaliana*. *Genes Genet. Syst.* **78**, 1–9.

Sakamoto, W., Tamura, T., Hanba-Tomita, Y. and Murata, M. (2002) The *VAR1* locus of *Arabidopsis* encodes a chloroplastic FtsH and is responsible for leaf variegation in the mutant alleles. *Genes Cells*, **7**, 769–780.

Sugimoto, H., Kusumi, K., Tozawa, Y., Yazaki, J., Kishimoto, N., Kikuchi, S. and Iba, K. (2004) The *virescent-2* mutation inhibits translation of plastid transcripts for the plastid genetic system at an early stage of chloroplast differentiation. *Plant Cell Physiol.* **45**, 985–996.

Surpin, M., Larkin, R.M. and Chory, J. (2002) Signal transduction between the chloroplast and the nucleus. *Plant Cell*, **14**, 327–338.

Takahashi, S. and Murata, N. (2008) How do environmental stresses accelerate photoinhibition? *Trends Plant Sci.* **13**, 178–182.

Tissier, T., Woolhead, C.A. and Robinson, C. (2002) Unique structural determinants in the signal peptide of ''spontaneously'' inserting thylakoid membrane proteins. *Eur. J. Biochem.* **269**, 3131–3141.

Wu, D., Wright, D.A., Wetzel, C., Voytas, D.F. and Rodermel, S. (1999) The *IMMUTANS* variegation locus of *Arabidopsis* defines a mitochondrial alternative oxidase homolog that functions during early chloroplast biogenesis. *Plant Cell*, **11**, 43–55.

Yamanouchi, U., Yano, M., Lin, H., Ashikari, M. and Yamada, K. (2002) A rice spotted leaf gene, *Spl7*, encodes a heat stress transcription factor protein. *Proc. Natl Acad. Sci. USA*, **99**, 7530–7535.

Yang, M., Wardzala, E., Johal, G.S. and Gray, J. (2004) The wound-inducible *Lls1* gene from maize is an orthologue of the *Arabidopsis Acd1* gene, and the LLS1 protein is present in non-photosynthetic tissues. *Plant Mol. Biol.* **54**, 175–191.

Yao, N. and Greenberg, J.T. (2006) *Arabidopsis* ACCELERATED CELL DEATH2 modulates programmed cell death. *Plant Cell*, **18**, 397–411.

Yoo, S.-C., Cho, S.-H., Sugimoto, H., Li, J., Kusumi, K., Koh, H.-J., Iba, K. and Paek, N.-C. (2009) Rice *Virescent3* and *Stripe1* encoding the large and small subunits of ribonucleotide reductase are required for chloroplast biogenesis during early leaf development. *Plant Physiol.* **150**, 388–401.

Yu, F., Fu, A., Aluru, M., Park, S., Xu, Y., Liu, H., Liu, X., Foudree, A., Nambogga, M. and Rodermel, S. (2007) Variegation mutants and mechanisms of chloroplast biogenesis. *Plant Cell Environ.* **30**, 350–365.

Zhang, H., Li, J., Yoo, J.-H., Yoo, S.-C., Cho, S.-H., Koh, H.-J., Seo, H.S. and Paek, N.-C. (2006) Rice *Chlorina-1* and *Chlorina-9* encode ChlD and ChlI subunits of Mg-chelatase, a key enzyme for chlorophyll synthesis and chloroplast development. *Plant Mol. Biol.* **62**, 325–337.

